TU/e EINDHOVEN UNIVERSITY OF TECHNOLOGY

Development of non-cell adhesive vascular grafts using supramolecular building blocks

Citation for published version (APA):
van Almen, G., Talacua, H., Ippel, B. D., Mollet, B., Ramaekers, M., Simonet, M., Smits, A. I. P. M., Bouten, C. V. C., Kluin, J., & Dankers, P. Y. W. (2016). Development of non-cell adhesive vascular grafts using supramolecular building blocks. *Macromolecular Bioscience*, *16*(3), 350-362. https://doi.org/10.1002/mabi.201500278

DOI:
10.1002/mabi.201500278

Document status and date:
Published: 01/01/2016

Document Version:
Publisher's PDF, also known as Version of Record (includes final page, issue and volume numbers)

Please check the document version of this publication:

• A submitted manuscript is the version of the article upon submission and before peer-review. There can be important differences between the submitted version and the official published version of record. People interested in the research are advised to contact the author for the final version of the publication, or visit the DOI to the publisher's website.
• The final author version and the galley proof are versions of the publication after peer review.
• The final published version features the final layout of the paper including the volume, issue and page numbers.

Link to publication

General rights
Copyright and moral rights for the publications made accessible in the public portal are retained by the authors and/or other copyright owners and it is a condition of accessing publications that users recognise and abide by the legal requirements associated with these rights.

• Users may download and print one copy of any publication from the public portal for the purpose of private study or research.
• You may not further distribute the material or use it for any profit-making activity or commercial gain
• You may freely distribute the URL identifying the publication in the public portal.

If the publication is distributed under the terms of Article 25fa of the Dutch Copyright Act, indicated by the "Taverne" license above, please follow below link for the End User Agreement:

www.tue.nl/taverne

Take down policy
If you believe that this document breaches copyright please contact us at:

openaccess@tue.nl

providing details and we will investigate your claim.

Download date: 23. Aug. 2022

Development of Non-Cell Adhesive Vascular Grafts Using Supramolecular Building Blocks

Geert C. van Almen, Hanna Talacua, Bastiaan D. Ippel, Björne B. Mollet, Mellany Ramaekers, Marc Simonet, Anthal I. P. M. Smits, Carlijn V. C. Bouten, Jolanda Kluin, Patricia Y. W. Dankers*

Cell-free approaches to in situ tissue engineering require materials that are mechanically stable and are able to control cell-adhesive behavior upon implantation. Here, the development of mechanically stable grafts with non-cell adhesive properties via a mix-and-match approach using ureido-pyrimidinone (UPy)-modified supramolecular polymers is reported. Cell adhesion is prevented in vitro through mixing of end-functionalized or chain-extended UPy-polycaprolactone (UPy-PCL or CE-UPy-PCL, respectively) with end-functionalized UPy-poly(ethylene glycol) (UPy-PEG) at a ratio of 90:10. Further char acterization reveals intimate mixing behavior of UPy-PCL with UPy-PEG, but poor mechanical properties, whereas CE-UPy-PCL scaffolds are mechanically stable. As a proof-of-concept for the use of non-cell adhesive supramolecular materials in vivo, electrospun vascular scaffolds are applied in an aortic interposition rat model, showing reduced cell infiltration in the presence of only 10% of UPy-PEG. Together, these results provide the first steps toward advanced supramolecular biomaterials for in situ vascular tissue engineering with control over selective cell capturing.

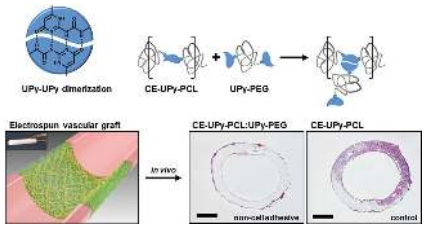

Dr. G. C. van Almen, B. D. Ippel, Dr. B. B. Mollet, Dr. M. Ramaekers, Dr. P. Y. W. Dankers
Department of Biomedical Engineering
Laboratory of Chemical Biology, and Institute for Complex Molecular Systems
Eindhoven University of Technology
P.O. Box 513 5600 MB, Eindhoven, The Netherlands
E-mail: p.y.w.dankers@tue.nl
H. Talacua, Dr. J. Kluin
Department of Cardio-Thoracic Surgery
University Medical Center Utrecht
3584 CX, Utrecht, The Netherlands
M. Simonet, Dr. A. I. P. M. Smits, Prof. C. V. C. Bouten
Department of Biomedical Engineering
Soft Tissue Biomechanics and Tissue Engineering
and Institute for Complex Molecular Systems
Eindhoven University of Technology
P.O. Box 513 5600 MB, Eindhoven, The Netherlands

1. Introduction

The growing clinical need for vascular substitutes boosts the research in the area of vascular tissue engineering. For small caliber vascular bypass grafts, autologous arteries and veins are the golden standard.[1] Since they are often not available or suitable due to the diseased state of the vessel wall, the development of synthetic grafts composed of poly(tetrafluoro ethylene) (PTFE) and poly(ethylene terephthalate) (Dacron) gained a lot of attention. However, a major limitation of these synthetic grafts when used as small caliber bypass grafts is their low patency due to intimal hyperplasia leading to occlusion of the graft.[2] Rapid endothelialization of the graft surface has been proven to reduce intimal hyperplasia.[3,4] Unfortunately, endothelialization of the graft in vitro prior to

© 2015 WILEY-VCH Verlag GmbH & Co. KGaA, Weinheim

DOI: 10.1002/mabi.201500278

implantation is time-consuming and costly, and therefore mutually exclusive with the increasing demand for 'off-the-shelf' solutions to treat acute vascular injuries. This has marked a shift from the classical tissue engineering strategy, which typically requires long culturing protocols in vitro,[5] via the implantation of preseeded vascular scaffolds in vivo,[6] toward an off-the-shelf approach using cell-free grafts that guide blood vessel formation in situ.[7]

In order to be applied successfully as a supporting scaffold for in situ vascular tissue engineering a biomaterial should be indistinguishable from the body, become fully resorbed after implantation, and interact with the biological environment to facilitate tissue regeneration.[8] Hence, the scaffold should be mechanically stable and provide cell-specific cues to attract and capture the required cell type, and direct their proliferative and migratory behavior. To this end most biomaterials are designed in order to closely mimic the native extracellular matrix (ECM) that provides structural support to the tissue and forms an environmental niche that determines cell fate.[9–11] This inspired researchers to design biomaterials consisting of biopolymers such as collagen, fibronectin or chitosan, and the application of decellularized vascular constructs (reviewed in[12]). These scaffolds provide the proper biological environment and matrix organization, but often lack the appropriate mechanical properties, and show batch to batch differences. Importantly, cross-linking strategies to improve mechanical performance often require cytotoxic conditions limiting a viable interaction with cells in these grafts, and therefore their widespread use in the clinic (reviewed in[12]). Synthetic materials on the other hand can be tuned with respect to degradation kinetics and physical properties, but are sometimes conflicting with biocompatibility and cause undesired cellular responses that limit their patency and vessel formation in vivo. One strategy to enhance cell-material interactions is biofunctionalization of the synthetic graft via immobilization of ECM-derived peptide sequences at the surface. Possibly the most featured peptide sequence is Arg-Gly-Asp (RGD), but also fibronectin-derived Pro-His-Ser-Arg-Asn (PHSRN) and Arg-Glu-Asp-Val (REDV), collagen-derived Asp-Gly-Glu-Ala (DGEA), and laminin-related Ile-Lys-Val-Ala-Val (IKVAV) and Tyr-Ile-Gly-Ser-Arg (YIGSR) recognition sequences have been incorporated into synthetic vascular scaffolds to improve graft patency[13,14] (reviewed in[4]). These approaches aim at inducing rapid endothelialization by promoting adhesion of endothelial cells and progenitor cells. Although promising results have been obtained, intimal hyperplasia leading to occlusion of the graft is often reported as a significant complication on the long term. It is posed that intimal hyperplasia is caused by random adhesion and migration of non-endothelial cell types within the graft.[15] This is not surprising, given the fact that in reality endothelial and circulating progenitor cells compete with various other cell types in vivo.[15] It is for this reason that we hypothesize that in order to fully guide the tissue engineering process via the recruitment of specific cell populations, we first need a non-cell adhesive surface to prevent immediate occlusion of the scaffold with various other cell types during the first phases after implantation.

Non-cell adhesive behavior can be introduced via poly(ethylene glycol) (PEG), which is the most commonly used polymer to reduce cell-adhesion on biomaterial surfaces and has successfully been applied in vivo.[16,17] An additional advantage of PEG as synthetic molecule for in vivo application is its high biocompatibility resulting from its hydrophilic nature.[18–20] However, simply blending of non-adhesive molecules into the bulk may result in unstable substrates due to phase separation within the material ultimately causing loss of non-adhesive surface properties in time.[21] To overcome this problem peptide- and PEG-linker molecules are covalently immobilized at the surface, which requires tedious synthetic procedures.[20] Therefore a simple method that enables the combination of different components to obtain a solid, mechanically stable, biomaterial without the need of complex preparation techniques is highly desirable. Supramolecular chemistry is proposed to be eminently suitable for the development of such controllable biomaterials, because various supramolecular modules can be mixed-and-matched to combine their specific properties into a single material. This provides a simple but powerful means to develop tunable materials that fulfill all requirements a biomaterial demands, based on its intended application. Strategies that combine multiple supramolecular units to introduce specific functionalities to a biomaterial are reported, but mainly involve hydrogel systems.[22–27] Unfortunately, their low mechanical strength make hydrogels unfavorable for application as a stand-alone vascular graft.

The objective of this study is to explore a modular strategy toward the development of a non-cell adhesive, mechanically stable material for application in vivo. To this end ureido-pyrimidinone (UPy)-modified[28] polymers were created consisting of end-modified bifunctional UPy-polycaprolactone (UPy-PCL)[29] and UPy-PEG,[29] and of chain-extended UPy-PCL (CE-UPy-PCL)[30] in which the UPy-moieties are part of the main chain (Figure 1). These UPy-groups are self-complementary hydrogen bonding units that are able to dimerize via four hydrogen bonds.[28] The reversible nature of these UPy-UPy dimers gives the material its dynamic properties, and importantly, enables blending of UPy-functionalized polymers according to a mix-and-match principle.

First a material screening approach was applied to establish the optimal ratio of UPy-PCL or CE-UPy-PCL

© 2015 WILEY-VCH Verlag GmbH & Co. KGaA, Weinheim

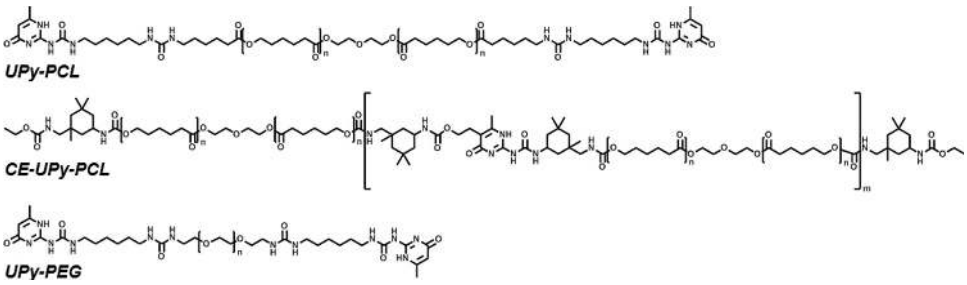

Figure 1. Supramolecular UPy-modified PCL and PEG polymers. The self-complementary UPy-moiety was coupled to prepolymers of PCL (2000 g mol^{-1}) and PEG (2000 g mol^{-1}) to obtain end-functionalized UPy-PCL (top), chain-extended UPy-PCL (middle), and end-functionalized UPy-PEG (bottom).

to UPy-PEG that yielded a surface that sufficiently prevented adhesion of endothelial cells and fibroblast in vitro.[31] To this end the well-defined UPy-PCL, which is known to form nanofibrous structures via stacking of dimerized UPy-units and adjacent urea functionalities, was intimately mixed with UPy-PEG at different weight ratios.[32,33] In a similar manner UPy-PEG was blended with CE-UPy-PCL, that was proposed to be mechanically more stable, but features less well-defined nanostructures due to the presence of a cyclic spacer that alters the dimerization behavior between UPy-moieties.[34,35] The morphology and wettability of the different surfaces where characterized using atomic force microscopy and water contact angle measurements, respectively. Subsequently, the non-cell adhesive conditions of UPy-PCL and CE-UPy-PCL with UPy-PEG where used to create two-dimensional fibrous meshes via electrospinning, and their mechanical performance was measured. Ultimately, as a proof-of-concept that non-cell adhesive supramolecular materials can be used in vivo, electrospun scaffolds of the mechanically strong CE-UPy-PCL were applied as vascular grafts in an aortic interposition model in rats followed by determination of the cellular ingrowth in the scaffolds at 4 and 48 h after implantation.[36]

2. Experimental Section

2.1. Supramolecular UPy-Polymers

UPy-PCL and UPy-PEG polymers were used (Figure 1). Commercially available PCL-diol (2000 g mol^{-1}) was end-functionalized or chain-extended, as described previously, to obtain end-functionalized UPy-PCL[29] and CE-UPy-PCL,[30,34] respectively. UPy-PEG was obtained via end-functionalization of PEG (2000 g mol^{-1}) as described.[29]

2.2. Preparation of Non-Cell Adhesive Surfaces

Drop cast supramolecular UPy-polymer surfaces were obtained via mixing of UPy-modified PCL polymers with UPy-PEG at different weight ratios. CE-UPy-PCL and UPy-PCL were dissolved in hexafluoroisopropanol (HFIP) (Acros Organics) (10% w/v solution) by stirring at room temperature for 16–24 h. In order to find the optimal UPy-PCL to UPy-PEG ratio, UPy-PEG was added to UPy-PCL and CE-UPy-PCL at a w/w ratio of 95:5, 90:10, 85:15, 80:20, and 75:25 (end-functionalized or chain-extended UPy-PCL:UPy-PEG). Each film contained 5 mg UPy-polymer and was cast from a volume of 50 µL 10% w/v polymer solution and dried overnight at room temperature followed by an additional 24 h in vacuo at 40 °C. Substrates were cast in an eight-well chamber slide (BD) for screening studies to identify the optimal UPy-polymer ratio, or on 13 mm round glass coverslips (Menzel Glaser) for quantification of adhered cell numbers. Prior to cell seeding all substrates were UV-sterilized for 30–60 min. Samples for infrared (IR) spectroscopy and water contact angle measurements were cast on 15 mm round glass cover slips (Menzel Glaser). Substrates for atomic force microcopy (AFM) were prepared in a similar manner and cast onto 15 mm round glass cover slips from 1 mg mL^{-1} polymer solutions in HFIP.

2.3. Cell Adhesion Studies In Vitro

Human umbilical vein endothelial cells (HUVEC) and mouse fibroblasts (NIH/3T3) were seeded on the polymer surfaces to identify non-cell adhesive conditions in vitro. Cell studies were performed at a density of 3–3.5 × 10^4 cells cm^{-2} under standard culturing conditions at 37 °C and 5% CO_2. HUVEC were obtained from Lonza and cultured according to the manufacturer's protocol; i.e., in EGM-2 medium supplemented with the required growth factors and antibiotics (EGM-2 Single Quots Bullitkit). 3T3 fibroblasts were cultured in Dulbecco's Modified Eagle Medium (DMEM), supplemented with 10% v/v fetal bovine serum (FBS) and 1% v/v penicillin and streptomycin (Invitrogen). In order to examine stability of the films and non-cell adhesive responses to a range of UPy-polymer blends containing varying amounts of UPy-PEG (0–25% w/w UPy-PEG), phase contrast images were made at 4 and 24 h after seeding, using a Zeiss Axiovert40C microscope equipped with a Canon PowerShot A650IS digital camera. Next, the number of adhering cells was evaluated and quantified for the polymer substrates that showed non-cell adhesive behavior and remained stable under culturing conditions. To this end, cytoskeletal actin fibers were stained with phalloidin 1, 3, and 7 d after seeding. HUVEC and NIH/3T3 fibroblasts were fixed for 15 min with 3.7% formaldehyde solution in phosphate buffered saline (PBS) at room temperature. After additional washing with PBS, cells were permeabilized and blocked for aspecific binding with 0.1% Triton X-100 and 4% normal horse

© 2015 WILEY-VCH Verlag GmbH & Co. KGaA, Weinheim

serum in PBS, followed by incubation with Phalloidin Atto-488 (Sigma-Aldrich, dilution 1:500 in PBS) for 30 min at room temperature. Cell nuclei were counterstained with 4′-6-diamidino-2-phenylindole (DAPI) (Invitrogen). Samples were mounted with Mowiol (Sigma) and analyzed with a Zeiss Axiovert 200M microscope and AxioVision software for quantification, and with two-photon confocal laser scanning microscopy (Zeiss LSM510 META NLO) and ZEN software for qualitative analysis. Cell nuclei were counted using MatLab (MathWorks, R2013b) to determine the number of adhered cells on the different polymer substrates. Three separate surfaces of each UPy-polymer blend were analyzed. The cell number of each individual substrate was determined from five different regions on that surface.

2.4. Atomic Force Microscopy

The morphology of the non-cell adhesive surfaces containing either end-functionalized or chain extended UPy-PCL mixed with 10% UPy-PEG was studied using AFM and compared to that of films cast from pristine UPy-PCL, CE-UPy-PCL, or UPy-PEG. AFM measurements were performed on a Digital Instrument Multimode Nanoscopy IV using PPP-NCHR-50 silicon cantilever tips in tapping mode at a scan rate of 1 Hz. After substrate preparation drop cast polymer surfaces were stored at room temperature under standard laboratory conditions for 1 week before AFM analysis was performed.

2.5. Infrared Spectroscopy

IR spectra of end-functionalized and chain-extended UPy-PCL:UPy-PEG blends were recorded on a Fourier transformed IR spectrometer (Perkin Elmer Spectrum Two, with a Universal ATR sampling Accessory and diamond crystal) in the range of 1400–1000 cm^{-1} at a resolution of 4 cm^{-1}.

2.6. Water Contact Angle Measurements

Water contact angle measurements were performed on an OCA30 contact angle system from DataPhysics in combination with SCA20 software to examine the wettability of the UPy-polymer surfaces. Water droplets with a volume of 5 μL were applied at a dosing rate of 1 μL min^{-1} to UPy-PCL and CE-UPy-PCL substrates with increasing percentages of UPy-PEG. Contact angles were determined at the polymer-air-water interface after 60 s. Three a samples were measured per condition and presented as the mean ± standard error of the mean (SEM).

2.7. Erosion of UPy-PEG: Release Experiments

The erosion of UPy-PEG from UPy-PCL:UPy-PEG and CE-UPy-PCL:UPy-PEG mixtures (weight ratio of 90:10) was determined in an aqueous environment. Drop cast films with a total polymer content of 5 mg were prepared from 10% w/v polymer solutions in HFIP, similar to the surfaces used for the in vitro cell adhesion studies, and subsequently exposed to 1 mL of water at 37 °C for 24 h. Dissolution of UPy-PEG from the bulk into the aqueous phase was determined by measuring the UV absorbance of the UPy-moiety at 220 nm on a Varian Cary 50 Scan UV–visible Spectrophotometer. A dilution series ranging from 2 to 100 μg mL^{-1} of UPy-PEG was prepared and confirmed a linear correlation between the concentration of UPy-PEG and the UV-absorbance. Next, samples were diluted accordingly, and the UPy-PEG concentration was deducted from the measured UV-absorbance with respect to the applied dilution factor.

2.8. Preparation of Electrospun Meshes

Meshes with ≈1–5 μm thick fibers were electrospun from end-functionalized and chain-extended UPy-PCL polymers with and without UPy-PEG using an in-house built electrospin setup. UPy-PCL meshes were prepared from 15% w/w polymer solution in HFIP. To create the mixed scaffold, UPy-PEG was mixed with UPy-PCL in a 90:10 w/w ratio (UPy-PCL:UPy-PEG) and electrospun from a 25% w/w polymer solution in HFIP. Both polymer solutions were electrospun at 18.5 kV, using a feed-rate of 0.020 mL min^{-1} and a tip-to-target distance of 12 cm. CE-UPy-PCL polymers were dissolved in a mixture of dichloromethane (DCM) and ethanol (EtOH) (volume ratio 3:1) to a 10% w/w polymer solution. In a similar manner UPy-PEG was mixed with CE-UPy-PCL in a 90:10 w/w ratio (CE-UPy-PCL:UPy-PEG) and dissolved in DCM/EtOH (10% w/w polymer solution). CE-UPy-PCL and CE-UPy-PCL:UPy-PEG materials were spun at 12 kV, using a feed rate of 0.025 mL min^{-1} and a tip-to-target distance of 15 cm. Fibers were deposited on a static, grounded collector plate that was covered with a polyethylene film to enable facile removal of the electrospun scaffold. Subsequently, the scaffolds were dried in vacuo at 40 °C for 16–24 h to remove residual solvent. Scaffold morphology was examined with scanning electron microscopy imaging using an FEI Quanta 600 and Xt Microscope Control software. Samples of comparable size and thickness were fixed on a metal stub using adhesive conductive carbon tape and imaged under high vacuum ($<1.3 \times 10$–4 mbar) conditions. Secondary electrons were detected with an accelerating voltage of 1–2 kV and a working distance of 10 mm.

2.9. Mechanical Characterization of Electrospun Meshes

Mechanical performance of the UPy-PCL and CE-UPy-PCL scaffolds with and without UPy-PEG was measured using a Biotester biaxial tensile tester (CellScale Biomaterial Testing) in air at room temperature. Local strains were determined using particle tracking of randomly applied graphite spots. Prior to tensile testing 7 × 7 mm samples were preconditioned with 10 cycles of 10% uniaxial strain in *x*- and *y*-direction sequentially, followed by similar straining conditions in biaxial direction and 60 s recovery between the straining protocols. After preconditioning, the Young's moduli in both *x*- and *y*-directions were determined from uniaxial tensile tests up to 10% strain, followed by equibiaxial straining at 25% to determine the yield point, and study the isotropic behavior of electrospun scaffolds. The Young's moduli were determined from the linear elastic region of the stress–strain curves, using the local strains.

2.10. Electrospinning of Tubular Grafts

Tubular scaffolds of CE-UPy-PCL and CE-UPy-PCL:UPy-PEG (mixed at weight ratio of 90:10) were prepared from 15% w/w

© 2015 WILEY-VCH Verlag GmbH & Co. KGaA, Weinheim

polymer solutions in a mixture of DCM and EtOH (volume ratio 3:1). All scaffolds were electrospun in a climate-controlled electrospinning cabinet (IME Technology, Geldrop, the Netherlands) equipped with a 14G nozzle and target rod (2 × 100 mm) rotating at 100 rpm to obtain a tube-like vascular graft with an internal diameter of 2 mm. CE-UPy-PCL and CE-UPy-PCL:UPy-PEG grafts were electrospun at 18 and 15 kV, respectively. The polymer solution feedrate was 0.010 mL min^{-1} and the tip-to-target distance was 15 cm. Electrospinning conditions were controlled at a temperature of 23 °C and 35% relative humidity. The fibrous nature and fiber diameter of the tubular scaffolds were examined with SEM as described in the previous section.

2.11. Non-Cell Adhesive Behavior of CE-UPy-PCL:UPy-PEG Scaffold Materials In Vivo

In order to study the biocompatibility and non-cell adhesive behavior in vivo, electrospun tubular grafts from CE-UPy-PCL with and without UPy-PEG were implanted and evaluated in a vascular interposition model in rats.[36] All animal studies were approved by the Institutional Animal Research Committee and conform to the guidelines for the use of laboratory animals as formulated by the Dutch law on care and use of experimental animals. Prior to surgery all rats were sedated with 2% isoflurane and received buprenorphine as postoperatively analgesia. Scaffolds of CE-UPy-PCL with 10% w/w UPy-PEG were placed in the abdominal aorta between the renal arteries and the aortic bifurcation. Control animals received a vascular graft consisting of pristine CE-UPy-PCL. $n = 4$ per group were evaluated. A Gore-Tex sheet separated the scaffold from the adjacent vasculature and surrounding tissues to inhibit the influx of non-circulating cells. Cellular infiltration and scaffold morphology were examined 4 and 48 h after implantation and compared to CE-UPy-PCL control grafts. Immediately after explanation, grafts were rinsed with sodium chloride solution and fixed in 10% formalin for 24 h, followed by pre-embedding in 1% (w/v) agar (Eurogentec). Paraffin embedded grafts were cut into 4 µm thick cross-sections and immunohistochemically stained with primary antibodies against CD68 (Serotec, MCA341GA, dilution 1:400) and myeloperoxidase (MPO) (Dako, A398, dilution 1:2000), followed by 2 h incubation with the secondary antibodies poly-HRP-conjugated antimouse (Immunologic) to detect CD68 and poly-HRP-conjugated anti-rabbit (Immunologic) for MPO detection. The number of cells residing in the scaffold was quantified from hematoxylin and eosin (HE) stained tissue sections. Additionally, the number of MPO positive granulocytes and $CD68^+$ macrophages was examined to determine the inflammatory response. For histochemical analyses, four representative areas were examined per tissue section at 400× magnification and quantified using ImageJ software.

2.12. Statistical Analysis

Data were presented as mean and standard error of the mean (SEM). Student's *t*-test was performed using GraphPad Prism software to compare experimental groups. A difference with a p value less than 0.05 was considered statistically significant.

3. Results and Discussion

3.1. Identification of Non-Cell Adhesive Conditions In Vitro

By functionalization of PCL and PEG with UPy-units, this study aimed at developing non-cell adhesive surfaces for cells by simple mixing of these two UPy-polymers (Figure 1). It was proposed that both polymers intimately mix because of the presence of the UPy-units in both polymers. In order to determine the optimal UPy-modified PCL:UPy-PEG ratio that prevented cell adhesion, UPy-PEG and one of each UPy-modified PCL polymer were mixed at various weight ratios; i.e., 95:5, 90:10, 85:15, 80:20, and 75:25 for either UPy-PCL or CE-UPy-PCL to UPy-PEG. Phase contrast microscopy showed impaired cell adhesion of HUVEC and 3T3 fibroblasts to UPy-PCL and CE-UPy-PCL substrates containing 10% w/w UPy-PEG within the first 4–24 h after seeding. (Figures S1 and S2 in the Supporting Information). Moreover, increasing the UPy-PEG content to 15% w/w or 20% w/w did not seem to further suppress cell adhesion, and at 25% w/w of UPy-PEG large clusters of aggregated non-adhered cells were observed in both UPy-PCL and CE-UPy-PCL films (Figures S1 and S2 in the Supporting Information). Note that the opaqueness of the CE-UPy-PCL films limits the analysis of cell adhesive behavior on these surfaces from phase contrast images (Figures S1 and S2 in the Supporting Information). Importantly, we also observed large holes in the films containing 20% w/w or more UPy-PEG within 24 h, especially for CE-UPy-PCL:UPy-PEG mixtures. This implies that the presence of UPy-PEG in the CE-UPy-PCL films affected their stability by causing disintegration of the films at higher percentages of UPy-PEG in an aqueous environment (Figure S1 in the Supporting Information). Therefore, it is proposed that the optimal non-cell adhesive surface comprises of the lowest percentage of UPy-PEG which still sufficiently prevents cell adhesion, but renders a stable material, which was considered at a 90:10 w/w ratio of UPy-modified PCL:UPy-PEG. In order to investigate whether these substrates maintain their non-cell adhesive properties over the course of one week, cell adhesion was determined 1, 3, and 7 d after seeding. After one day the number of adhered HUVEC and 3T3 fibroblasts on UPy-PEG containing surfaces was reduced compared to substrates of UPy-PCL and CE-UPy-PCL alone (Table 1). Additional actin-phalloidin staining revealed the formation of multiple actin-fibers in HUVEC and 3T3 fibroblasts grown on pristine UPy-PCL and CE-UPy-PCL, whereas the few HUVEC and 3T3 fibroblasts that remained at the films containing UPy-PEG lack the formation of these fibers (Figures 2 and 3). Instead, cells grown on UPy-PEG modified surfaces show impaired cytoskeletal organization and the formation of multiple actin-rich lamellopodia, which hallmarks

© 2015 WILEY-VCH Verlag GmbH & Co. KGaA, Weinheim

Table 1. Cell adhesion of HUVEC and 3T3 fibroblasts to UPy-modified PCL substrates with and without UPy-PEG.

	UPy-PCL	UPy-PCL:UPy-PEG	CE-UPy-PCL	CE-UPy-PCL:UPy-PEG
HUVEC				
1 d	148 ± 11	0017 ± 5[a)]	192 ± 33	099 ± 26[b)]
3 d	158 ± 20	0059 ± 7[a)]	155 ± 19	216 ± 23
7 d	346 ± 87	126 ± 9	286 ± 25	444 ± 81
Fibroblast				
1 d	413 ± 44	0015 ± 8[a)]	365 ± 75	042 ± 3[c)]
3 d	n.d.	006 ± 2	n.d.	n.d.
7 d	n.d.	030 ± 5	n.d.	n.d.

The number of adhered HUVEC and 3T3 fibroblasts was determined at five different locations per substrate. After 3 d, fibroblasts entered a superconfluent stage on UPy-PCL, CE-UPy-PCL, and CE-UPy-PCL:UPy-PEG and formed a dense multilayer for which the cell number could not be quantified reliebly and was therefore indicated as not determined (n.d.). $N = 3$ substrates per condition. Data are presented as mean ± S.E.M. cells mm^{-2}.
[a)] $P \leq 0.05$ versus UPy-PCL; [b)] $P = 0.1$ versus CE-UPy-PCL; [c)] $P \leq 0.05$ versis CE-UPy-PCL.

non-adhered cells (Figures 2 and 3). Importantly, this non-cell adhesive behavior was maintained after 3 and 7 days for UPy-PCL:UPy-PEG, but not for CE-UPy-PCL:UPy-PEG. After 3 and 7 d the number of residing HUVEC was not significantly different between pristine CE-UPy-PCL and CE-UPy-PCL:UPy-PEG (Table 1). This indicates that CE-UPy-PCL:UPy-PEG loses its non-cell adhesive properties within the first 3 d. This might be related to the disintegration of these substrates after incorporation of UPy-PEG, whereas the UPy-PCL:UPy-PEG blend shows stable non-cell adhesive behavior over the course of 7 d. Moreover, these effects were even more pronounced for 3T3 fibroblasts, that showed a rapid increase in cell number between day 1 and day 3 resulting in the formation of a dense multilayer of fibroblasts on UPy-PCL, CE-UPy-PCL and CE-UPy-PCL:UPy-PEG, but not on UPy-PEG modified UPy-PCL surfaces (Figure 3). The overgrowth of 3T3 fibroblasts observed after 3 and 7 days is related to the lack of contact inhibition in this cell

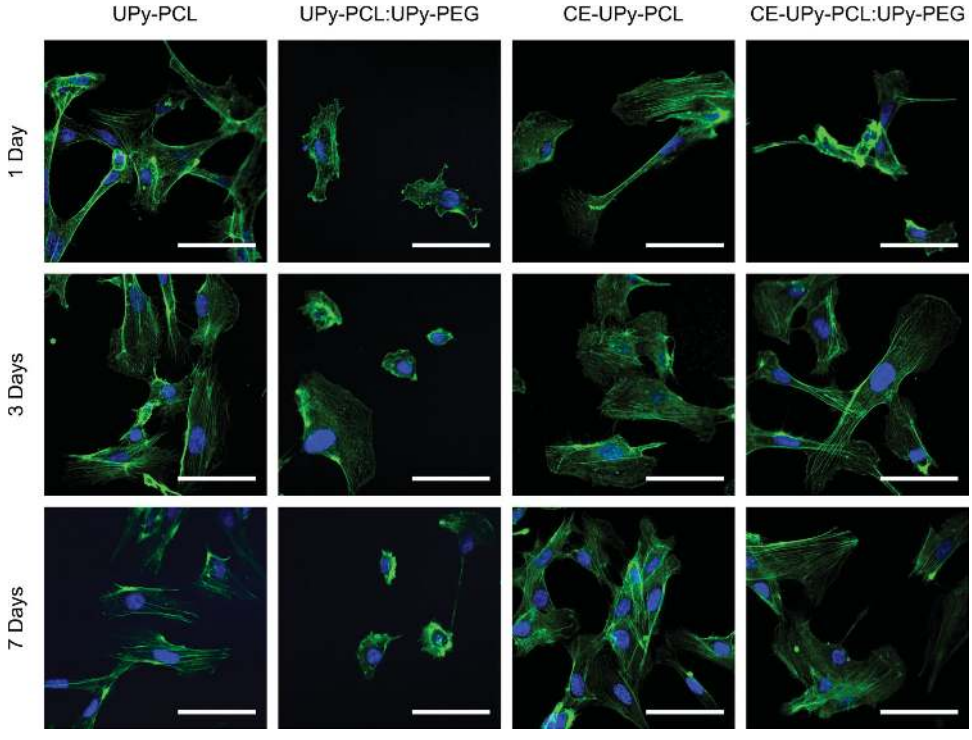

Figure 2. Characterization of cytoskeletal actin organization. Fluorescent actin phalloidin staining of human umbilical vein endothelial cells (HUVEC) 1, 3, and 7 d after seeding on UPy-PCL and CE-UPy-PCL drop cast films. UPy-PCL:UPy-PEG and CE-UPy-PCL:UPy-PEG were prepared at a weight ratio of 90:10. Scale bars represent 50 µm.

© 2015 WILEY-VCH Verlag GmbH & Co. KGaA, Weinheim

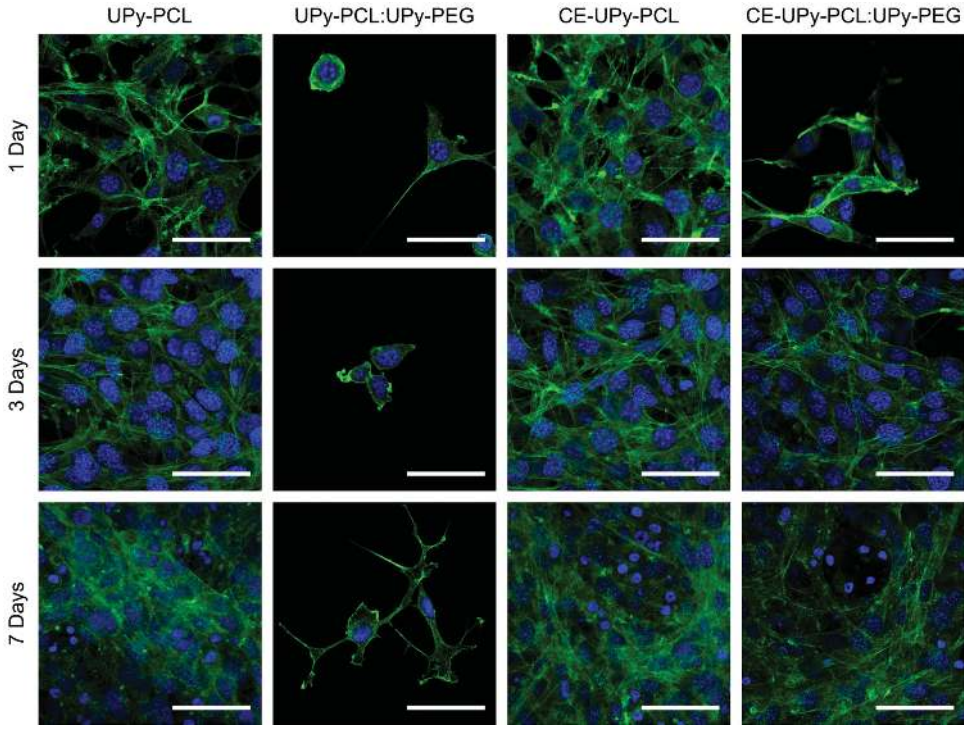

Figure 3. Characterization of cytoskeletal actin organization. Fluorescent actin phalloidin staining of 3T3 fibroblasts 1, 3, and 7 d after seeding on UPy-PCL and CE-UPy-PCL drop cast films. UPy-PCL:UPy-PEG and CE-UPy-PCL:UPy-PEG were prepared at a weight ratio of 90:10. Scale bars represent 50 μm.

type and impeded a reliable quantitative analysis of the number of adhered cells (Table 1).

Considering the above, it is concluded that simple mixing of UPy-modified PCL polymers with UPy-PEG at a ratio of 90:10 (UPy-PCL:UPy-PEG) is feasible to create stable surfaces that prevent initial cell adhesion within the first 24 h in vitro. However the long-term non-cell adhesive effects of the UPy-polymer blends seem to depend on the nature of the UPy-modified PCL polymer; i.e., a mixture of UPy-PEG with the well-defined end-functionalized UPy-PCL showed a prolonged non-cell adhesive effect as compared to a polymer blend comprising the less well-defined CE-UPy-PCL. Nevertheless, these findings are in line with other studies that also reported non-cell adhesive behavior after grafting of PEG onto a surface in vitro[37,38] or as a stent surface coating to prevent unwanted cell-material interactions after implantation.[39,40]

Alternatively, block copolymers that comprise a PEG segment allow easy processing into fibrous substrates. The first study to address this problem was performed by Grafahrend et al. who demonstrated non-cell adhesive properties of electrospun fibrous substrates that were created from a block copolymer of PEG-block-poly(ε-caprolactone).[41] They also showed that introduction of an amphiphilic macromolecule based on star-shaped poly(ethylene oxide) into poly(D,L-lactide-*co*-glycolide) meshes suppressed cell material interactions in vitro due to increased hydrophilicity of the electrospun fibers.[42] Furthermore, supramolecular host-guest chemistry based on cyclodextrin-adamantane complexes has recently been shown to be suitable to fine-tune the cell-adhesive properties of a PCL substrate in vitro by simple adjusting the complexation ratio of adamantane-functionalized PEG to the cyclodextrin immobilized surface.[43]

3.2. Characterization of Supramolecular UPy-Polymer Surfaces

After identification of the optimal UPy-PCL or CE-UPy-PCL to UPy-PEG ratio (90:10) that prevented cell adhesion in vitro, the morphology of these non-cell adhesive surfaces was characterized. AFM micrographs of UPy-PCL and UPy-PEG showed nanofibrous structures which are composed of UPy-dimers that are stacked in the lateral direction via π-π interactions and additional hydrogen bonding between the urea groups (Figure 4a, height images are presented in Figure S3 in the Supporting Information).[33,44] Similar nanofibrous structures were observed upon mixing of UPy-PCL with 10% UPy-PEG suggesting that both UPy-polymers are supramolecularly mixed (Figure 4a). On the contrary, the surface of CE-UPy-PCL films was characterized by large PCL crystalline domains, lacking a fibrous morphology (Figure 4a). This implied that the UPy-moieties did not assemble into

© 2015 WILEY-VCH Verlag GmbH & Co. KGaA, Weinheim

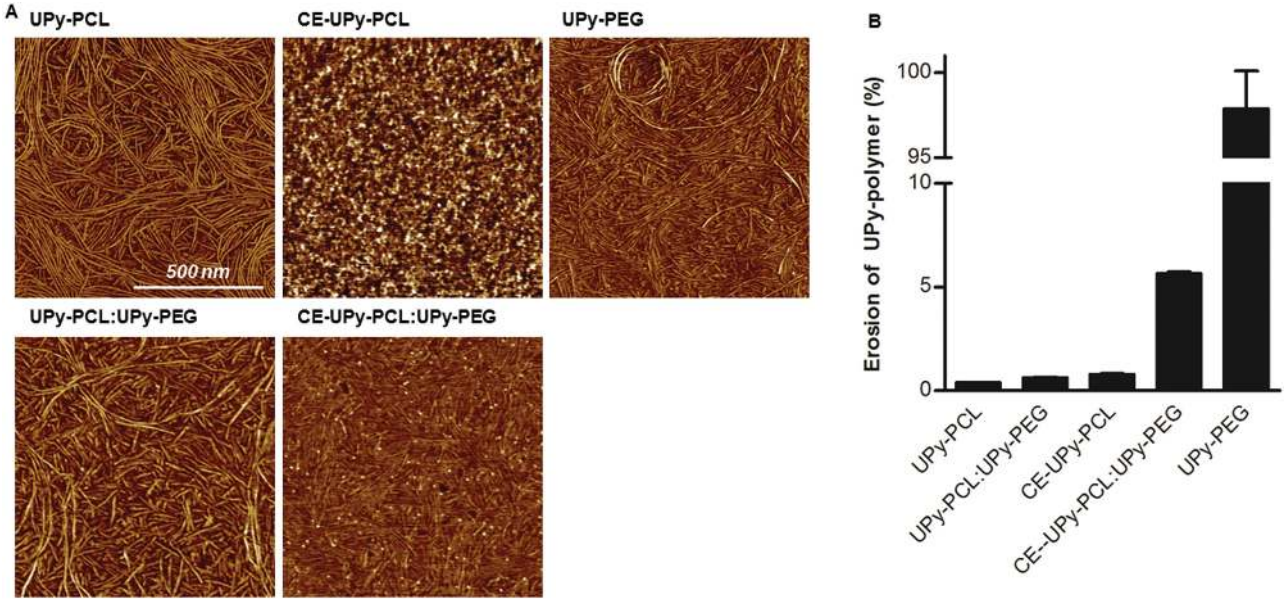

Figure 4. A) Atomic force microscopy phase images of pristine UPy-PCL, CE-UPy-PCL, and UPy-PEG drop cast surfaces, and of both UPy-modified PCL polymers mixed with 10% UPy-PEG. Scale bars represent 500 nm B) Erosion of UPy-PEG from UPy-modified PCL:UPy-PEG drop cast substrates in water after 24 h. Erosion of UPy-PEG is presented relative to the bulk (5 mg of total UPy-polymer was used per drop cast). Data are presented as mean ± S.E.M. All UPy-modified PCL:UPy-PEG surfaces were prepared at a weight ratio of 90:10.

nanofibers. It is proposed that in this case inter- and intramolecular UPy-dimerization occurred that resulted in the formation of less well-defined small aggregates that were not visible with AFM. This is proposed to be due to the cyclic isophorone spacer and the ability of PCL to crystallize.[35] Importantly, upon introduction of UPy-PEG in CE-UPy-PCL small nanofibers were observed (Figure 4a). This showed that either UPy-PEG induced fiber formation in CE-UPy-PCL by co-assembly, or that both UPy-polymers phase separated, and UPy-PEG thereby assembled in nanofibers that became visible at the surface. This data suggests that UPy-PCL and UPy-PEG can be supramolecularly mixed, whereas CE-UPy-PCL and UPy-PEG are less well mixed.

The presence of UPy-PEG is determined with IR spectroscopy showing that the ratio of the C–O vibrations at 1108 and 1160 cm^{-1}, of the ether versus ester groups, respectively, changes upon increasing the UPy-PEG content in both UPy-PCL and CE-UPy-PCL (Figure S4 in the Supporting Information). This confirms the presence of UPy-PEG in both UPy-modified PCL polymer mixtures. Water contact angle measurements showed the presence of UPy-PEG at the surface by demonstrating enhanced wettability of UPy-PCL and CE-UPy-PCL substrates when mixed with different percentages of UPy-PEG. Similar contact angles of 67.0°±0.4° and 67.1°±0.2° were obtained for the pristine UPy-PCL and CE-UPy-PCL surfaces, respectively (Table 2). Gradually increasing the UPy-PEG content from 5% to 25% in end-functionalized UPy-PCL films coincided with a stepwise decrease in the contact angle from 52.7°±0.2° to 38.9°±1.1°, respectively (Table 2). The hydrophilic behavior of CE-UPy-PCL:UPy-PEG surfaces was characterized by a dramatic lowering of the contact angle upon mixing with 5% and 10% UPy-PEG to 27.4 ± 0.5° and 22.2 ± 0.6°, respectively. Increasing the UPy-PEG content to 15% or higher did not result in a further reduction of the contact angle (Table 2). Interestingly, surfaces comprised of UPy-PEG alone demonstrated a contact angle of 35.0°±1.0° which is higher than the contact angles reported for CE-UPy-PCL:UPy-PEG blends (Table 2). On the

Table 2. Contact angle (Θ) at the air-water-material interface of UPy-modified PCL:UPy-PEG surfaces.

	Water contact angle [Θ] in degrees [°][a]	
	UPy-PCL	**CE-UPy-PCL**
UPy-modified PCL	67.0 ± 0.4	67.1 ± 0.2
UPy-modified PCL:UPy-PEG (ratio)		
95:5	52.7 ± 0.2	27.4 ± 0.5
90:10	48.0 ± 0.5	22.2 ± 0.6
85:15	41.9 ± 0.8	18.9 ± 1.0
80:20	42.6 ± 0.4	21.3 ± 0.9
75:25	38.9 ± 1.1	21.7 ± 0.8
UPy-PEG	35.0 ± 1.0	

[a]Contact angles are indicated as the mean angle of three different locations on a drop cast polymer film and the standard error of the mean. Contact angles are measured after 60 s.

© 2015 WILEY-VCH Verlag GmbH & Co. KGaA, Weinheim

contrary, increasing the UPy-PEG content in the end-functionalized UPy-PCL materials also reduced the contact angles, but never below the angle reported for UPy-PEG alone (Table 2). These differences in wettability between both UPy-modified PCL polymers after mixing with UPy-PEG are in line with the distinct morphologies of UPy-PCL and CE-UPy-PCL observed with AFM, and support the notion that incorporation of UPy-PEG in the chain-extended material is different than in the end-functionalized UPy-PCL materials.

3.3. Erosion of UPy-PEG from the Surface

Cell studies showed a marked difference between UPy-PCL:UPy-PEG and CE-UPy-PCL:UPy-PEG materials in the ability to maintain their non-cell adhesive behavior over time. In order to study whether the differences in morphology and wettability between UPy-PCL and CE-UPy-PCL affects the retention of the highly water-soluble UPy-PEG in the material, erosion of UPy-PEG from the bulk was examined. Importantly, UPy-PCL and CE-UPy-PCL are insoluble in water, indicating that the observed UV-absorbance correlated to dissolution of UPy-PEG (Figure S5a–c in the Supporting Information). Importantly, less than 1% w/w of the total UPy-PCL:UPy-PEG material was lost due to erosion, whereas CE-UPy-PCL:UPy-PEG mixtures demonstrated a loss of 5.6% w/w of UPy-polymer (Figure 4b). Considered that UPy-modified PCL polymers are insoluble in an aqueous environment and films comprised of pristine UPy-PEG dissolved completely (Figure 4b and Figure S5d in the Supporting Information), these data indicated that less than 6% of the total UPy-PEG content eroded from the UPy-PCL:UPy-PEG surface, whereas more than 56% of the UPy-PEG polymer was lost within 24 h when mixed with CE-UPy-PCL (Figure 4b). These results show that UPy-PEG is not fully retained in the material when blended with the chain-extended system presented here, and imply that possible phase separation of the two UPy-polymers contributes to dissolution of UPy-PEG from the surface. Mixing-and-matching of end-functionalized UPy-polymers on the other hand diminished erosion of UPy-PEG as a result of the intimate mixing with UPy-PCL. These results are in line with our cell studies showing loss of non-cell adhesive properties in CE-UPy-PCL:UPy-PEG substrates after 1 day. Moreover, the enhanced erosion of UPy-PEG from CE-UPy-PCL:UPy-PEG surfaces, supports the notion that the differences in morphology and wettability between both UPy-modified PCL polymers after blending with UPy-PEG affect the performance as a non-cell adhesive material.

3.4. Mechanical Performance of Electrospun UPy-Modified PCL:UPy-PEG Scaffolds

Successful application of a material for in situ vascular tissue engineering requires a fibrous scaffold that provides sufficient mechanical support after implantation. Therefore both pristine UPy-modified PCL polymers, and the non-cell adhesive mixtures identified in vitro were processed into fibrous meshes. Electrospun meshes of UPy-PCL and CE-UPy-PCL had a fiber diameter of 0.2–1.1 and 2.6–4.5 μm, respectively (Figure S6a in the Supporting Information and Figure 5a, respectively). Importantly, fiber dimensions were not significantly changed upon mixing with 10% UPy-PEG (0.4–1.3 μm in mixtures with UPy-PCL, and 0.9–3.6 μm in mixtures with CE-UPy-PCL) as compared to meshes comprised of either pristine UPy-PCL or CE-UPy-PCL (Figure S6b in the Supporting Information and Figure 5b, respectively). Mechanical properties of the electrospun UPy-PCL and CE-UPy-PCL materials were determined via biaxial tensile testing of meshes with comparable size and thickness, and revealed a marked difference in the mechanical performance of the two UPy-polymers (Figure 5a and Figure S6c in the Supporting Information). Electrospun UPy-PCL ruptured before tensile stress was applied, and therefore could not be measured, indicating that end-functionalized UPy-PCL materials are too brittle to be applied as vascular graft (Figure S6c,d in the Supporting Information). CE-UPy-PCL meshes on the other hand demonstrated good mechanical properties compared to the end-functionalized UPy-PCL scaffolds (Figure 5a,b). The Young's modulus of CE-UPy-PCL meshes in *x*- and *y*-direction was 11.9 MPa and 12.3 MPa, respectively, and the obtained yield stress was 0.6 MPa in both directions, illustrating the isotropic behavior of the scaffold (Table S1 in the Supporting Information). Importantly, addition of UPy-PEG to the chain-extended material did not significantly change the mechanical performance of the scaffold (Figure 5b and Table S1 in the Supporting Information). These results demonstrate the poor mechanical properties of end-functionalized UPy-PCL meshes, and therefore favor the mechanically well-performing CE-UPy-PCL material for load-bearing applications in vivo, such as a vascular scaffold.

3.5. Non-Cell Adhesive Behavior of Tubular Grafts In Vivo

Cell adhesion studies demonstrated non-cell adhesive behavior of UPy-PEG modified materials toward HUVEC and 3T3 fibroblasts during the first 24 h in vitro. For application as a graft material for in situ tissue engineering it is highly desirable to prevent immediate population of the scaffold with non-endothelial cell types that compete with endothelial progenitor cells in the circulation during the acute phase after implantation. Moreover, it is postulated that adverse remodeling that leads to fibrosis and stenosis of the graft can be prevented by carefully guiding the immediate-early cellular response that forms the basis of the formation of functional endothelialized autologous vascular tissue.[15] In order to validate the application of

© 2015 WILEY-VCH Verlag GmbH & Co. KGaA, Weinheim

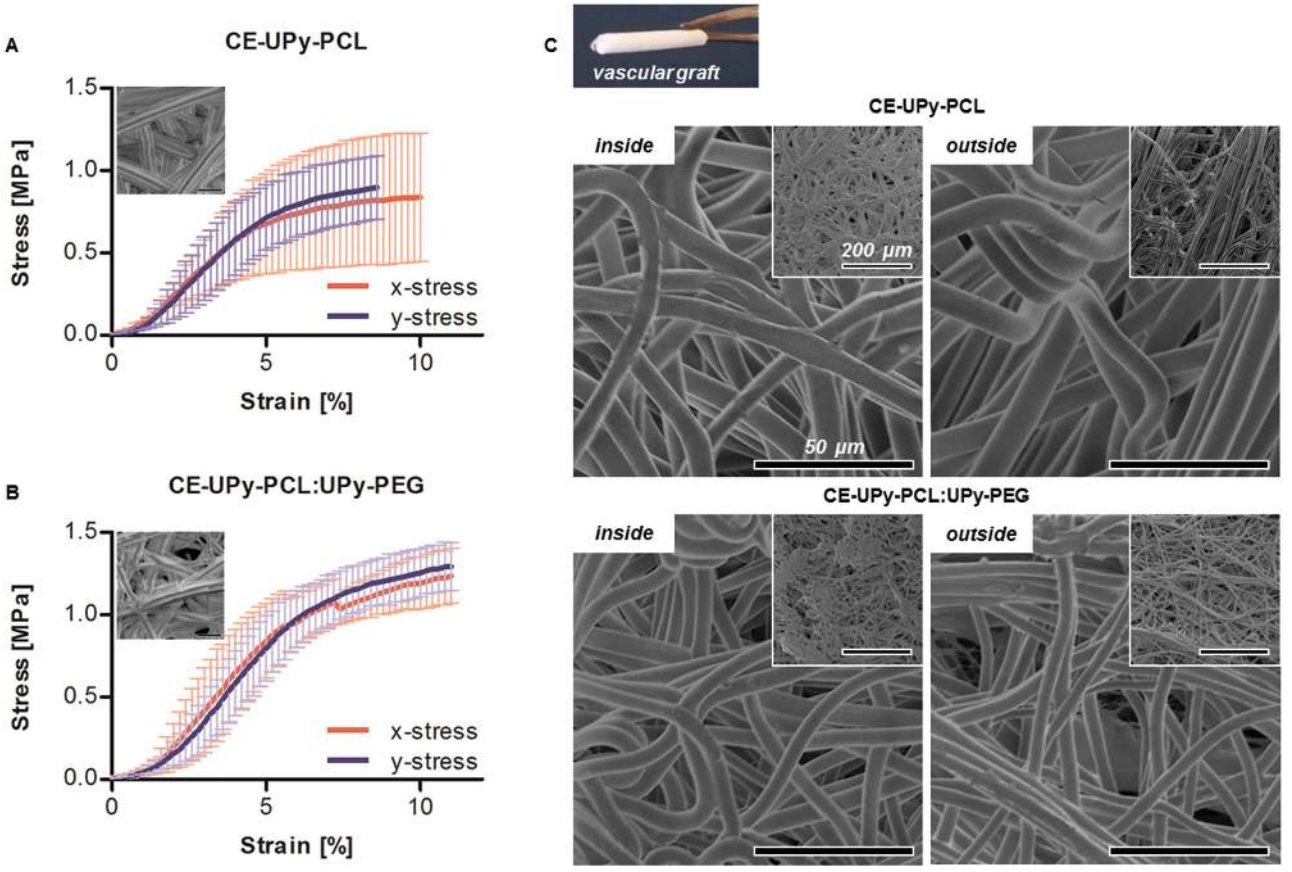

Figure 5. Biaxial tensile testing of electrospun A) CE-UPy-PCL and B) CE-UPy-PCL:UPy-PEG and representative SEM images of the electrospun scaffolds (panels (A) and (B), inset; scale bars represent 5 µm). Stress–strain curves represent the average of $n = 4$ scaffolds per condition. (C) SEM images of the inside (lumen) and outside of electrospun vascular grafts (top) from CE-UPy-PCL and CE-UPy-PCL:UPy-PEG (ratio 90:10). Scale bars represent 50 µm.

our supramolecular materials in vivo, electrospun CE-UPy-PCL tubular scaffolds were made, and the non-cell adhesive properties of these UPy-PEG-modified materials were examined during the first phases after implantation. To this end, vascular grafts were made of the CE-UPy-PCL material and implanted as an interposition graft in the abdominal aorta of a rat for 4 and 48 h.[36] Vascular grafts with an internal diameter of 2 mm were electrospun from CE-UPy-PCL and compared to non-cell adhesive scaffolds containing 10% UPy-PEG (Figure 5c). Electrospun vascular scaffolds were obtained with a fiber diameter ranging from 7.0 to 11.0 µm in CE-UPy-PCL grafts, and 3.9 to 7.0 µm in the UPy-PEG containing scaffolds (Figure 5c). Importantly, CE-UPy-PCL and CE-UPy-PCL:UPy-PEG grafts demonstrated non-fused, micrometer thick fibers on the inner (luminal) and outer side of the scaffold, indicating an open fibrous structure that is preferred for vascular tissue engineering in situ (Figure 5c). Implantation of the vascular grafts was performed successfully and all animals survived during the course of the study. Importantly, the scaffold provided sufficient strength for suturing and leak-free connection to the adjacent aortic ends, and no clinical signs of distant thromboemboli, such as a lowered temperature and decreased strength in de hind limbs, were observed upon implantation of the grafts. Macroscopic examination of the vascular grafts 4 and 48 h after implantation revealed reduced clot formation in the presence of UPy-PEG (Figure 6a). Moreover, histological analysis showed significant reduction in cellularity in UPy-PEG containing grafts compared to pristine CE-UPy-PCL (Figure 6b,c), indicating enhanced non-cell adhesive behavior in the presence of UPy-PEG. In order to study whether the increased cellularity in CE-UPy-PCL scaffolds was related to an enhanced acute inflammatory response triggered by the material, the number of infiltrating granulocytes and macrophages was determined by immunohistochemical staining for their cell specific markers MPO and CD68, respectively. Quantitative analysis showed a trend toward an increased number of MPO and CD68 positive cells in grafts that lacked UPy-PEG, but this did not reach significance. Together with the low grade inflammatory response seen in non-cell adhesive grafts these results imply that an enhanced early immune response, characterized by granulocytes and macrophages, did not contribute to the higher cellularity observed in

© 2015 WILEY-VCH Verlag GmbH & Co. KGaA, Weinheim

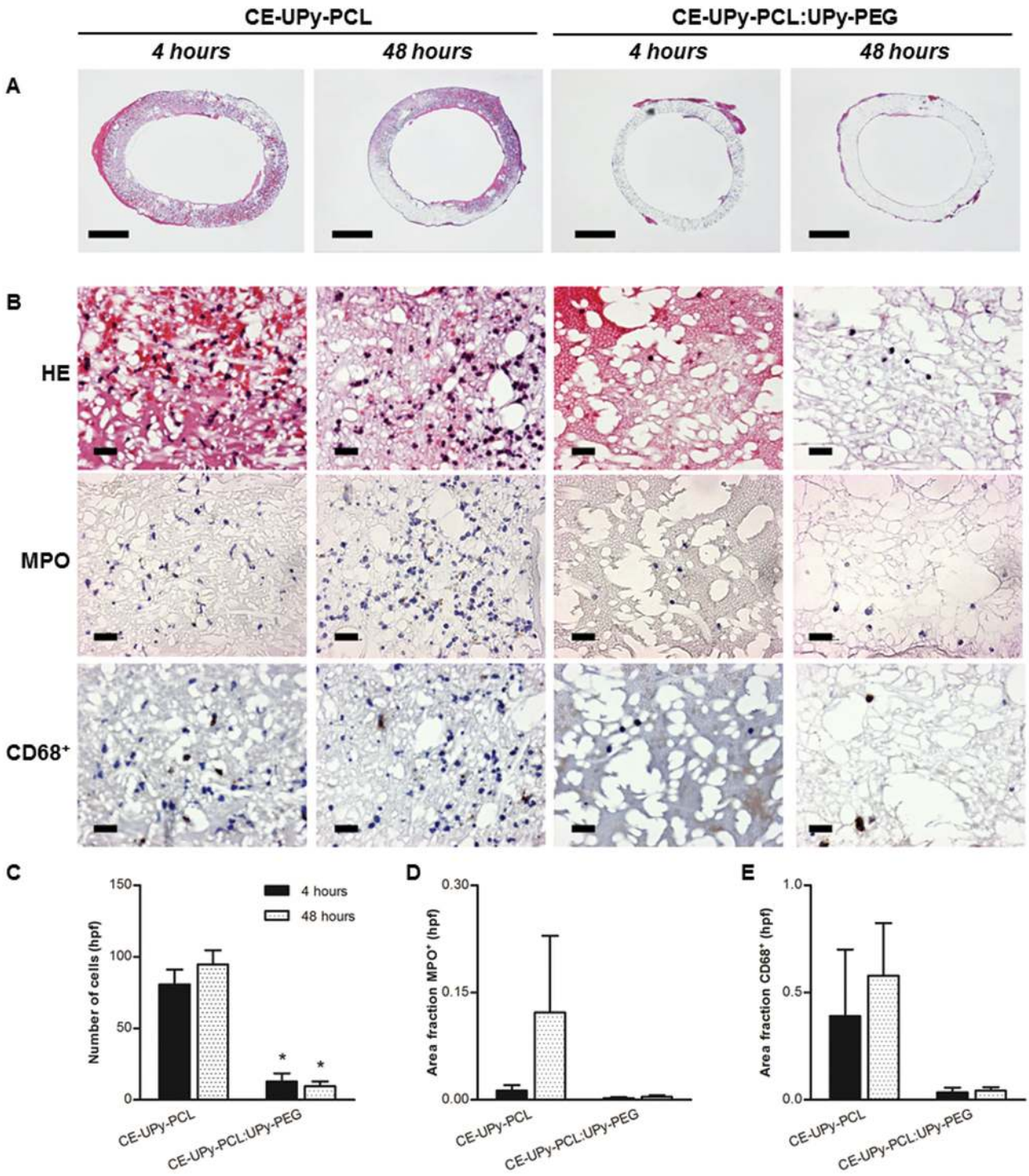

Figure 6. A) Cross sectional slices of HE stained vascular grafts after implantation for 4 and 48 h. Scale bars represent 500 µm. B) Representative images of HE stained (top) and immunohistochemical MPO (middle) and CD68 (bottom) stained tissue sections. Scale bars represent 20 µm. C) Histological analysis showed reduced cellularity in CE-UPy-PCL:UPy-PEG vascular grafts. Quantitative analysis of the area of D) MPO positive granulocytes and E) CD68+ macrophages relative to the total tissue area. Bar graphs represent infiltrating cell number quantified from four representative high power fields (hpf) per tissue section analyzed at 400× magnification. Data are presented as mean ± S.E.M.

CE-UPy-PCL (Figure 6b,d,e). Importantly, these results are in line with our findings in vitro, and showed that mixing of CE-UPy-PCL with UPy-PEG also reduced cell adhesion in a vascular graft in vivo. Thereby, this study for the first time proofs the concept of a modular approach using supramolecular UPy-modified polymers to create a mechanically

© 2015 WILEY-VCH Verlag GmbH & Co. KGaA, Weinheim

stable, non-cell adhesive biomaterial that can be applied in vivo by simple mixing of UPy-PEG with CE-UPy-PCL.

After gaining control over mechanical performance and nonspecific cell adhesion within cell-free vascular grafts, as shown in this study, incorporation of a third, bioactive component into our currently still non-cell adhesive supramolecular material is a prerequisite to ultimately enable specific bioactivation of our vascular scaffold. Application of the modular approach might contribute to such advanced biomaterials via integration of different functionalities through mixing-and-matching of supramolecular UPy-polymers. Importantly, previous studies from our group have proven the concept of bioactivating UPy-polymer materials through the introduction of UPy-functionalized ECM-peptides.[29,32,45]

4. Conclusions

This proof-of-concept study demonstrates that a modular approach using supramolecular UPy molecules provides a powerful, but simple approach to create non-cell adhesive scaffolds with good mechanical properties that can be applied in vivo. Incorporation of a third, bioactive component that adds control over cell-specific material interactions is subject to current studies and opens new avenues for the development of advanced bioactive materials for in situ vascular tissue engineering in the future.

Supporting Information

Supporting Information is available from the Wiley Online Library or from the author.

Acknowledgements: The authors thank A. W. Bosman from SupraPolix BV for providing the CE-UPy-PCL compound, H. M. Janssen from SyMO-Chem BV for the UPy-PCL compound, A. J. H. Spiering for the synthesis of the UPy-PEG material, and A. Nandakumar from Xeltis BV for technical assistance. The authors alos thank E. W. Meijer, F. P. T. Baaijens, E. Burakowska-Meise, and M. Cox (Xeltis BV) for useful discussions. The research leading to these results received funding from the Ministry of Education, Culture and Science (Gravity program 024.001.035), the Netherlands Organisation for Scientific Research (NWO), and the European Research Council (FP7/2007–2013) ERC Grant Agreement 308045. This research forms part of the Project P1.01 iValve of the research program of the BioMedical Materials institute, co-funded by the Dutch Ministry of Economic Affairs. The financial contribution of the Netherlands Heart Foundation is gratefully acknowledged.

Received: July 23, 2015; Revised: October 8, 2015; Published online: November 27, 2015; DOI: 10.1002/mabi.201500278

Keywords: biomaterials; non-cell adhesive behavior; supramolecular polymers; vascular grafts

[1] M. A. Cleary, E. Geiger, C. Grady, C. Best, Y. Naito, C. Breuer, *Trends Mol. Med.* **2012**, *18*, 394.
[2] R. Y. Kannan, H. J. Salacinski, P. E. Butler, G. Hamilton, A. M. Seifalian, *J. Biomed. Mater. Res., Part B* **2005**, *74*, 570.
[3] Q. Lin, X. Ding, F. Qiu, X. Song, G. Fu, J. Ji, *Biomaterials* **2010**, *31*, 4017.
[4] A. De Mel, G. Jell, M. M. Stevens, A. M. Seifalian, *Biomacromolecules* **2008**, *9*, 2969.
[5] L. E. Niklason, J. Gao, W. M. Abbott, K. K. Hirschi, S. Houser, R. Marini, R. Langer, *Science* **1999**, *284*, 489.
[6] B. Udelsman, N. Hibino, G. A. Villalona, E. McGillicuddy, A. Nieponice, Y. Sakamoto, S. Matsuda, D. A. Vorp, T. Shinoka, C. K. Breuer, *Tissue Eng., Part C* **2011**, *17*, 731.
[7] G. Matsumura, N. Nitta, S. Matsuda, Y. Sakamoto, N. Isayama, K. Yamazaki, Y. Ikada, *PLoS One* **2012**, *7*, e35760.
[8] L. L. Hench, J. M. Polak, *Science* **2002**, *295*, 1014.
[9] A. J. Engler, S. Sen, H. L. Sweeney, D. E. Discher, *Cell* **2006**, *126*, 677.
[10] N. Huebsch, P. R. Arany, A. S. Mao, D. Shvartsman, O. A. Ali, S. A. Bencherif, J. Rivera-Feliciano, D. J. Mooney, *Nat. Mater.* **2010**, *9*, 518.
[11] M. M. Stevens, J. M. George, *Science* **2005**, *310*, 1135.
[12] J. P. Stegemann, S. N. Kaszuba, S. L. Rowe, *Tissue Eng.* **2007**, *13*, 2601.
[13] W. Zheng, Z. Wang, L. Song, Q. Zhao, J. Zhang, D. Li, S. Wang, J. Han, X. -L. Zheng, Z. Yang, D. Kong, *Biomaterials* **2012**, *33*, 2880.
[14] M. Nakamura, M. Mie, H. Mihara, M. Nakamura, E. Kobatake, *Biomaterials* **2008**, *29*, 2977.
[15] Y. Wei, Y. Ji, L.-L. Xiao, Q. Lin, J. Xu, K. Ren, J. Ji, *Biomaterials* **2013**, *34*, 2588.
[16] D. Lazos, S. Franzka, M. Ulbricht, *Langmuir* **2005**, *21*, 8774.
[17] Park Kinam, S. Shim Hong, K. Dewanjee Mrinal, L. Eigler Neal, *J. Biomater. Sci., Polym. Ed.* **2000**, *11*, 1121.
[18] N. Faucheux, R. Schweiss, K. Lützow, C. Werner, T. Groth, *Biomaterials* **2004**, *25*, 2721.
[19] M. Zhang, X. H. Li, Y. D. Gong, N. M. Zhao, X. F. Zhang, *Biomaterials* **2002**, *23*, 2641.
[20] Z.-K. Xu, F.-Q Nie, C. Qu, L.-S Wan, J. Wu, K. Yao, *Biomaterials* **2005**, *26*, 589.
[21] H. Chen, M. A. Brook, H. Sheardown, *Biomaterials* **2004**, *25*, 2273.
[22] J. D. Hartgerink, E. Beniash, S. I. Stupp, *Proc. Natl. Acad. Sci. USA* **2002**, *99*, 5133.
[23] S. Ghanaati, M. J. Webber, R. E. Unger, C. Orth, J. F. Hulvat, S. E. Kiehna, M. Barbeck, A. Rasic, S. I. Stupp, C. I. Kirkpatrick, *Biomaterials* **2009**, *30*, 6202.
[24] J. Z. Gasiorowski, J. H. Collier, *Biomacromolecules* **2011**, *12*, 3549.
[25] K. Rajangam, H. A. Behanna, M. J. Hui, X. Han, J. F. Hulvat, J. W. Lomasney, S. I. Stupp, *Nano Lett.* **2006**, *6*, 2086.
[26] M. E. Davis, J. P. M. Motion, D. A. Narmoneva, T. Takahashi, D. Hakuno, R. D. Kamm, S. Zhang, R. T. Lee, *Circulation* **2005**, *111*, 442.
[27] E. Genové, C. Shen, S. Zhang, C. E. Semino, *Biomaterials* **2005**, *26*, 3341.
[28] R. P. Sijbesma, F. H. Beijer, L. Brunsveld, B. J. B. Folmer, J. H. K. K. Hirschberg, R. F. M. Lange, J. K. L. Lowe, E. W. Meijer, *Science* **1997**, *278*, 1601.
[29] B. B. Mollet, M. Comellas-Aragones, A. J. H. Spiering, S. H. M. Söntjens, E. W. Meijer, P. Y. W. Dankers, *J. Mater. Chem. B* **2014**, *2*, 2483.
[30] P. Y. W. Dankers, G. M. L. van Gemert, H. M. Janssen, E. W. Meijer, A. W. Bosman(SupraPolix BV), *EP 1877113*, **2008**.

© 2015 WILEY-VCH Verlag GmbH & Co. KGaA, Weinheim

[31] S. W. Cranford, J. de Boer, C. van Blitterswijk, M. J. Buehler, *Adv. Mater.* **2013**, *25*, 802.
[32] P. Y. W. Dankers, J. M. Boomker, A. Huizinga-van der Vlag, E. Wisse, W. P. J. Appel, F. M. M. Smedts, M. C. Harmsen, A. W. Bosman, E. W. Meijer, M. J. A. van Luyn, *Biomaterials* **2011**, *32*, 723.
[33] H. Kautz, D. J. M. Havermans-van Beek, R. P. Sijbesma, E. W. Meijer, *Macromolecules* **2006**, *39*, 4265.
[34] P. Y. W. Dankers, E. N. M. van Leeuwen, G. M. L. van Gemert, A. J. H. Spiering, M. C. Harmsen, L. A. Brouwer, H. M. Janssen, A. W. Bosman, M. J. A. van Luyn, E. W. Meijer, *Biomaterials* **2006**, *27*, 5490.
[35] S. H. M. Söntjens, R. A. E. Renken, G. M. L. van Gemert, T. A. P. Engels, A. W. Bosman, H. M. Janssen, L. E. Govaert, F. P. T. Baaijens, *Macromolecules* **2008**, *41*, 5703.
[36] H. Talacua, A. I. P. M. Smits, D. E. P. Muylaert, J. W. van Rijswijk, A. Vink, M. C. Verhaar, A. Driessen-Mol, L. A. van Herwerden, C. V. C. Bouten, J. Kluin, F. P. T. Baaijens, *Tissue Eng., Part A* **2015**, (in press).
[37] Y. Nakayama, M. Miyamura, Y. Hirano, K. Goto, T. Matsuda, *Biomaterials* **1999**, *20*, 963.
[38] K. Mougin, M. B. Lawrence, E. J. Fernandez, A. C. Hillier, *Langmuir* **2004**, *20*, 4302.
[39] H. J. Lee, J.-K. Hong, H. C. Goo, W. K. Lee, K. D. Park, S. H. Kim, Y. M. Yoo, Y. H. Kim, *J. Biomater. Sci., Polym. Ed.* **2002**, *13*, 939.
[40] M. Billinger, F. Buddeberg, J. A. Hubbell, D. L. Elbert, T. Schaffner, D. Mettler, S. Windecker, B. Meier, O. M. Hess, *J. Invasive Cardiol.* **2006**, *18*, 423.
[41] D. Grafahrend, J. Lleixa Calvet, J. Salber, P. D. Dalton, M. Moeller, D. Klee, *J. Mater. Sci.: Mater. Med.* **2008**, *19*, 1479.
[42] D. Grafahrend, K.-H. Heffels, M. V. Beer, P. Gasteier, M. Möller, G. Boehm, P. D. Dalton, J. Groll, *Nat. Mater.* **2011**, *10*, 67.
[43] Q. Ji, S. Zhang, J. Zhang, Z. Wang, J. Wang, Y. Cui, L. Pang, S. Wang, D. Kong, Q. Zhao, *Biomacromolecules* **2013**, *14*, 4099.
[44] E. Wisse, A. J. H. Spiering, P. Y. W. Dankers, B. Mezari, P. C. M. M. Magusin, E. W. Meijer, *J. Polym. Sci., Part A: Polym. Chem.* **2011**, *49*, 1764.
[45] P. Y. W. Dankers, M. C. Harmsen, L. A. Brouwer, M. J. A. Van Luyn, E. W. Meijer, *Nat. Mater.* **2005**, *4*, 568.

© 2015 WILEY-VCH Verlag GmbH & Co. KGaA, Weinheim